LC-MSMS OF PERMETHYLATED N-GLYCANS DERIVED FROM MODEL AND HUMAN BLOOD SERUM GLYCOPROTIENS

Yunli Hu, Tarek Shihab and Yehia Mechref*

Department of Chemistry and Biochemistry, Texas Tech University, Lubbock, TX 79409

Running Title: LC-MS of Permethylated Glycans

*Corresponding author

Department of Chemistry and Biochemistry

Texas Tech University

Lubbock, TX 79409-1061

Email: yehia.mechref@ttu.edu

Tel: 806-742-3059

Fax: 806-742-1289

Keywords: Glycans, Glycoproteins, Permethylation, LC-MS, LC-MSMS.

Abstract

LC-MS/MS is one of the most powerful tools for N-glycan structure elucidation. However, it is still challenging to identify some glycan structures with low abundance. In this study, we investigated the chromatogram behavior of permethylated N-glycans. The relationship between retention times *vs.* molecular weight of dextran, dextrin and model glycans and was investigated. Also, non-polar surface area (NPSA) of glycans was calculated and compared with experimental retention time. The trends of these are two similar when intermolecular interaction was included into calculation. Moreover, the retention time is corresponding to glycan types and branch types. Then, the N-glycans analysis model, which combining the use of high mass accuracy and retention time was applied to confirm serum N-glycans. Totally, there were 78 N-glycans compositions indentified. The linear relationship was observed for each subgroups. For example, R^2 for complex types N-glycans were better than 0.98. Moreover, the retention time could be further applied to distinguish structure isomers as well as linkage isomers. MSMS data was used to confirm the structure isomers.

Introduction

Glycosylation is one of the most common posttranslational modifications of proteins, since protein glycosylation attributes to many biological processes such as protein folding, transport, and targeting.[1] Moreover, aberrant glycosylation has been linked to the development of many human diseases, including cancer, inflammation and many immune diseases.[2,3] Therefore, glycans could be potentially utilized as biomarkers for disease diagnosis and prognosis. As such, characterization of glycosylation is a research area that has recently attracted a lot of attention.

Among the various analytical methods routinely employed for glycomics analysis, mass spectrometry (MS) has proven to be one of the most powerful tools because of its ability to produce a wealth of reliable data, allowing the analysis of glycans associated with complex biological samples. MS has been recently employed to elucidate glycan structures and their roles in disease progression.[4-7] However, structural elucidation remains a challenge in glycomics studies. Currently, the most reliable analytical tool for structural elucidation is tandem MS (MS^2 and MS^n) analysis, which provides structural information, thus allowing unequivocal glycan structural assignment.[8-13] Despite the wealth of information provided by MS^2 analysis, it is still challenging to identify some glycan structures, as there are not enough fragments produced to prompt effective identification. This ambiguity can be somewhat resolved through MS^3, or in some cases through MS^n analysis. However, MS^n analysis is not attainable in cases where the abundances of glycans are very low. Additionally, glycan concentration dynamic range within one sample can extend over several orders of magnitude, prompting detector bias which severely limits tandem MS capabilities. For glycans existing at low concentrations, chromatographic or electrophoretic separations overcome such limitations and generate reliable MS^n acquisitions.

Glycans of complex samples are effectively identified and characterized by combining liquid chromatography (LC) and MS. Recently, an LC method employing amide based columns was devised to analyze heterogeneous glycan mixtures.[14] The retention times of fluorescently labeled glycans were initially correlated to the retention times of dextran linear oligosaccharides to determine GU values. Such values were subsequently employed to deduce the structures of unknown glycans. Amide-modified nanocolumns have also been used to separate underivatized N-glycans for MS analysis.[15] Additionally, porous graphitic carbon columns interfaced to MS have been applied to separate and identify N-glycan isomeric structures.[16-18] Most of the recent studies employing this chromatography medium focused on structural identification of native glycans. However, one issue encountered when using mass spectrometry for the analysis of native glycans is the low ionization efficiency of such structures, especially in the case of sialylated glycans. The simultaneous detection of both acidic and neutral glycans in positive-mode MS is analytically challenging. This problem is easily addressed through the permethylation of N-glycans.[19-21] Not only can all of the permethylated glycans be observed in positive mode, but the ionization efficiency and stability of sialylated glycans is substantially improved as a result of permethylation.

In this study, we attained the separation of permethylated N-glycans using a C_{18} nanocolumn that is interfaced to an Orbitrap mass spectrometer to investigate the relationship between retention time and glycan structure. The chromatographic separation allowed the identification of glycan structures by their specific retention times. Also, the chromatographic separation allowed the confirmation of the majority of glycan structures commonly observed in human blood serum (HBS). A comprehensive 2-D map was generated and subsequently employed to determine the glycan structures associated with different samples. The above described LC-MS method

permitted a simplified characterization and unequivocal structural assignments of glycan structures associated with complex biological samples such as HBS.

Experimental

***Materials*.** Dextran, dextrin, model glycoprotein (including ribonuclease B (RNase B), fetuin and HBS were obtained from Sigma-Aldrich (St. Louis, MO). Other chemicals such as borane-ammonium complex, sodium hydroxide beads, dimethylsulfoxide, methyl iodide, trifluoroacetic acid, chloroform, and MS-grade formic acid were also purchased from Sigma-Aldrich. Microspin columns and graphitized carbon and C_{18} microspin columns were purchased from Harvard Apparatus (Holliston, MA). Acetic acid and HPLC-grade solvents, including methanol and isopropanol, were procured from Fisher Scientific (Pittsburgh, PA), while acetonitrile was obtained from JT Baker (Phillipsburg, NJ). HPLC grade water was acquired from Mallinckrodt Chemicals (Phillipsburg, NJ). Endoglycosidase purified from Flavobacteriummeningosepticum (PNGase F, 500,000 units/ml) was obtained from New England Biolabs Inc. (Ipswich, MA). Neuraminidase from clostridium perfringens was purchased from Sigma-Aldrich.

Methods

N-glycans Released from Model Glycoproteins. Stock solutions of model glycoproteins (10 μg/μL concentrations), including RNase B and fetuin were prepared. A 1-μL aliquot of each of the model glycoprotein stock solutions was mixed with a 9-μL aliquot of G7 buffer (50 mM sodium phosphate buffer, pH 7.5) provided by the vendor. Next, a 1-μL aliquot of a diluted PNGase F solution (prepared by diluting the vendor stock solution 10-times with G7 buffer) was added to each of the model glycoprotein solutions. The unit concentration of the diluted PNGase F solution is 50 units/μL. The reaction mixtures were then incubated for 18 hours at 37^{o}C in a

water bath (Thermo Scientific, Pittsburgh, PA). Upon the completion of the enzymatic digestion, samples were dried under vacuum (Labconco, Kansas City, MO).

N-glycans Released from HBS Glycoproteins. A 90-μL aliquot of denaturation phosphate buffer saline (PBS, consisting of 10mM sodium phosphate, 10 mM sodium chloride, 4 mM dithriothritol (DTT), 0.5% sodium dodecyl sulfate (SDS), pH 7.5) was added to a 10-μL aliquot of HBS. The sample was then incubated at 60^{o}C for 45 minutes and allowed to reach room temperature. This is employed to prompt partial denaturation of glycoproteins which permits efficient enzymatic release of N-glycans. A 5-μL aliquot of 10% aqueous NP-40 solution was added to consume free SDS. Next, a 2.4-μL aliquot of PNGase F (120 units) was then added prior to placing the sample in a 37^{o}C water bath for 18h. Next, a 690-μL aliquot of 5% acetonitrile (0.1% trifluoroacetic acid) was added to the enzymatically released glycans and centrifuged at 10K rpm for 30 min. The samples were then purified with charcoal microspin columns. First, the charcoal spin columns were washed with 100% ACN. Then, the column was washed with a 400-μL aliquot of 85% aqueous ACN solution. This step was repeated twice. Next, columns were conditioned with 400 μL of 5% aqueous ACN solution twice. The samples were then applied to the columns and the columns were washed five times with 5% aqueous ACN solution. Finally, glycans were eluted from the column using 200 μL of 40% aqueous ACN solution. This elution step was repeated twice, prior to mixing all eluants in a clean vial and drying under vacuum.

Desialylation of N-glycans from fetuin. N-glycans released from fetuin were also desialylated as described here. A 5-μL aliquot of enzymatically released fetuin was adjusted to pH 6.5 with 0.1 M hydrochloric acid. Next, a 1-μL aliquot of neuraminidase (1 μg/μL concentration, 0.01 unit)

was added to the sample and incubated at 37^{o}C for 4h. This was performed to generate non-siaylatedbiantennary and triantennary complex glycan compositions.

Reduction of N-glycans. A 10-μL aliquot of aqueous borane-ammonium complex (10 μg/μL concentration) was added to dextran, dextrin and the N-glycans enzymatically released from fetuin, RNase B, HBS, and neuraminidased treated fetuin. Each sample was then incubated in a 60^{o}C water bath for 1 hour prior to the addition of 10 μL of 5% acetic acid. Samples were then dried under vacuum. Next, a 100-μL aliquot of HPLC-grade methanol was added to form volatile methyl borate. The samples were then dried under vacuum. The last two steps were repeated several times to ensure effective elimination of excess borate introduced through the reduction reaction.

Solid-Phase Permethylation of N-glycans. Reduced glycans were permethylated using solid-phase permethylation according to the previously published method.[19-21] First, microspin columns were filled to 3 cm depth with sodium hydroxide beads and washed twice with 50-μL aliquots of DMSO. The dried and reduced glycan samples were resuspended in 1.2 μL water and 30 μL DMSO. A 20-μL aliquot of methyl iodide was then added to the sample prior to the application of the sample to the sodium hydroxide packed microspin column. The samples were allowed to sit for 30 minutes before the addition of another 20-μL aliquot of methyl iodide. The samples were then allowed to sit for an additional 20 minutes before centrifuged at 1.6K rpm. Finally, the sodium hydroxide columns were washed with 50 μL ACN twice to elute all permethylated glycans.

Solid-phase Purification of Permethylated N-Glycans. Solid-phase C_{18} cartridges (Harvard Apparatus, Holliston, MA) were used for purification of permethylated N-glycans prior to LC-MS/MS analyses. A 400-μL aliquot of 80% aqueous ACN solution were applied to C_{18} columns

and centrifuged. This was repeated twice. The cartridges were then washed with 400 µL of 100% ACN. Next, the cartridges were washed with 5% aqueous ACN solution. Permethylated samples were suspended in 690-µL aliquots of 5% aqueous ACN solution prior to loading to the cartridges. The columns were then washed three times with 400-µL aliquots of 5% aqueous ACN solutions. The cartridges were placed in clean eppendorf tubes prior to elution with 200-µL aliquot of 80% aqueous ACN solution. This step was repeated twice and the eluants were then collected in one vial and dried under vacuum. The dried samples were resuspended in 20% aqueous ACN solution containing 0.1% formic acid prior to MS analyses.

LC-MS and LC-MSMS. A Dionex 3000 Ultimate nano-LC system (Dionex, Sunnyvale, CA) was used for LC-MS analysis. The LC separation was attained under gradient conditions from 38%-45% solvent B over 32 min at flow rate of 350 nL/min. Solvent A consisted of 2% acetonitrile and 98% water with 0.1% formic acid, while solvent B consisted of acetonitrile and 0.1% formic acid. Acclaim® PepMap capillary column (150 mm x 75 µm i.d) packed with 100 Å C_{18} bounded phase (Dionex) was used for sample separation. Velos LTQ Orbitrap hybrid mass spectrometer (Thermo Scientific, San Jose, CA) was used for detection. The mass spectrometer was operated in an automated data-dependent acquisition mode in which the scan mode switched between MS full scan (m/z from 500-2000) and CID MS/MS scan which was conducted on the 8 most abundant ions with a 0.250 Q-value, 20 ms activation time, and 35% normalized collision energy.

Data evaluation. Xcarlibur Qual Browser (Thermo Fisher Scientific) was used for LC/ESI-MS data processing. Retention times of glycans were read from extracted ion chromatograms, which were generated using the isotopic masses of glycans with 10 ppm mass tolerance. A seven-point

boxcar smoothing was enabled to improve peak quality. Peak height was used to represent the abundance of a glycan structure.

Results and Discussion

The nonpolar surface area (NPSA) is the surface sum over all nonpolar atoms, primary carbon and hydrogen. Nonpolar driving forces of proteins were well studied for fundamental insights of protein folding and protein binding reactions.[22,23] Due to the hydrophilic property of native glycans, the nonpolar surface area is not well investigated. Hydrophobic tagging of glycans, including hydrazone formation, permethylation and peracetylation, has shown enhanced mass spectrometric ionization and detection.[24,25] Permethylation serves to render hydrophobicity to glycans, thus allowing separation on the C_{18} column. In this study, we correlated NPSA value to experimental retention time to better understand the chromatographic behavior of permethylated N-glycan. NPSA values of glycans were calculated to determine the optimal condition of chromatography and applied to estimate the retention time of unknown glycans as well as identify structural isomers.

Dextran is a branched glucan composed of chains of varying lengths while dextrin is a linear low-molecular-weight carbohydrate. Here, we use dextran and dextrin as model glucan to study the relationship between molecular weight and retention time as well as glucose unit with retention time. To further study how the branching of N-glycans influence the retention time, we mixed the reduced permethylated fetuin and desialylated fetuin and evaluated the chromatographic behavior of the different glycans present in such a mixture. **Figure 1** illustrates the relationship between retention time and glucose unit as well as the relationship between estimated NPSA and glucose unit for dextrin and N-glycans derived from fetuin. The estimated NPSA of a glycan is calculated using the assumption that the additional intermolecular forces

that arise with glycan branching cause the loss of availability of functional groups that would otherwise be available to interact with the C_{18} column.[25] With the increase of glucose unit, the retention time as well as NPSA was increased. And the trends of retention time and NPSA were similar; both of them show linear increasing. Moreover, retention time and NPSA value also related to the branch of glycans. With the increase of branch, the retention time and NPSA value decreased. **Table S1** summarizes the intensity and retention time of dextran, dextrin, and the mixed fetuin. When retention time *vs.* molecular weight (**Figure S2a**) or the retention time *vs.* glucose unit (**Figure S2b**) was plotted, a linear like relationship can be observed. As shown in **Figure S2** and **Table S1**, the retention times of linear glucans are lower than those of branched glucans for the same molecular weights. This might be due to the chain conformation of dextrin and dextran, both of which can be regarded as helical in various states of extension. Thus, for linear carbohydrates such as dextrin, the methyl groups inside the helix are not available for hydrophobic interaction with C_{18} column. However, the hydrophobicity of dextran increased with the increase in the number of branch glucose units outside and inside the helix. For fetuin, the retention times of triantennary glycans are lower than those of biantennary glycans for the same glucose unit or molecular weight. The interaction between branched glucose units resulted in the decrease of the glycan hydrophobicity. Moreover, the retention times of fetuin glycans appear to be substantially lower than their dextrin or dextran counterpart, even when the molecular weight is the same. The methyl groups associated with the permethylated fetuin N-glycans are not completely available for interacting with chromatographic media, which caused lower retention on the C_{18} column, whereas the methyl groups on the linear and partially linear structures appeared to be more available for interaction.

N-glycans derived from RNase B were further used as N-glycan models to demonstrate the possibility of using retention time as a structural indicator. **Figure S1** compared the retention time and glucose unit as well as the relationship between estimated NPSA and glucose unit for dextrin and high mannose glycans. The retention time as well as NPSA increased with the increase of glucose unit. **Figure S3** depicts the extracted ion chromatograms of RNase B. Five unique compositions of RNase B (Man5, Man6, Man7, Man8, Man9) were observed and their intensities varied from Man5 to Man9. The retention time and the molecular weight have a great linear relationship, as evidenced by an R^2 value of 0.998. The similar trend was discussed in the previous publication with R^2 value of 0.993.[26]

We applied the N-glycans analysis model, which is based on the use of high mass accuracy and retention time to confirm serum N-glycans. First, MS full scan was analyzed and all possible N-glycans were extracted based on accurate mass (**Figure 2**). The total compositions determined by mass accuracy (less than 2 ppm) were 78 (**Table S2**). We compared our results to those previously published by several groups,[27-31] more compositions especially unique compositions are confirmed by our work (**Table S3**). N-glycan structures in this study were also confirmed through MS/MS. Among the total detected glycans, 52 had sufficient MS/MS data for structural confirmation. Thus, identifying other compositions based on retention time and accurate mass is of great importance. Based on the results obtained from dextrin, dextran and N-glycans extracted from model glycoproteins, molecular weight, glycan structure and branching plays an important role in the retention time. Total N-glycans confirmed in serum were then divided into several groups based on glycan types and antennary. The relationship between retention time and molecular weight was investigated (**Figure 2**). In the case of mannose type glycans derived from HBS, the linear fit of the retention time demonstrated an R^2 value of 0.996 (**Figure 2b**), which is

comparable to that obtained for RNase B glycans. Although Man 9 derived from HBS has no MSMS for structure confirmation, we can determine the structure based on the retention time and mass accuracy. Complex N-glycans were classified into biantennary, triantennary tetraantennary and multiantennary subclasses. Also, for each subclass, they can be divided into several subgroups based on the Gal moities. As the increase of Gal moieties, the intermolecular interaction increased, thus the interaction of methyl group with C_{18} column decreased. From the equation, the slope remains the similar and the intercept decreased with the increase of the Gal moieties. This matches our assumption, intermolecular interaction contributes to the retention time. This phenomenon can be observed from biatennary, triatennary and tetraantennary complex type N-glycans. Generally, the retention time increases as molecular weight increases, and there is a good linear relationship with each subclass. For example, the R^2 values of biantennary glycans with one and two Gal moieties are 0.987 and 0.994 (**Figure 2c).** The triantennary glycans with one, two and three Gal moieties have an R^2 value of 0.999, 0.998 and 0.994, respectively (**Figure 2d)**. On the other hand, the influence of fucosylation to the retention time is subtle when the fucosylated sites are less than two. However, the multifocusylated glycans have lower retention time compared to their own antennary group (**Figure 2e)**. This can be explained with the stereo-hindrance effect, less methyl groups were available for interaction with C_{18} column. When it comes to sialic acid N-glycans, the similar phenomenon were observed. When the sialic acid unites increased to four, the retention times of them were decreased (**Figure 2e)**. The hybrid type N-glycans can be also divided into groups based on the antennary, too. Biantennary hybrid glycans has the R^2 of 0.990, when the compositions with multiantennary show a linear relationship with R^2 of 0.953. The relatively low R^2 partially due to the detected number is low for each subtype to study the relationship of molecular weight and

retention time **(Table S2)**. Also, in one subgroup, there are different branches. For example, both H6N3 and H6N4F1 could be triantennary hybrid glycans. H6N3 has two mannose branch when H6N4F1 has two complex branch, thus, they are not fit in a same line.

According to the above discussion, retention time can be used to predict N-glycans structure. For example, at the composition of H6N5S1 and H6N5S2, there are two peaks with equal masses extracted from chromatography. The H6N5S1 of chromatography peak at 25.93 min fit the line of triantennary subgroup, which indicates the structure type. And for peak of retention time at 27.5 min, the elution position fell consistent with other hybrid glycans. Similar to H6N5S1, H6N5S2 has two peaks from extracted chromatogram. The one with lower retention time fit the line of triantennary subgroup. MSMS data was interpreted for structural elucidation (**Figure 4**). The intensity of MSMS peaks varies from each other, there are few diagnostic peak for us to confirm the structure. This difference in conformation can be elucidated based on it's expected relationship between estimated NPSA and retention time, whose standard is developed from the glucan models. The N-glycans with the composition of H6N5F1S1 and H6N5F1S2 have three total peaks each. This is attributes to multiple positional attachment and linkage attachment. However, the specific structures cannot be discerned from tandem MSMS due to the lack of high collision energy to prompt cross ring fragments.

Conclusions

In this study, a new method was developed for confirming the compositions of reduced permethylated N-glycans based on retention time and molecular weight. Previous studies were mostly based on MS/MS, but as a result of the variability of glycan structure, MS/MS data must be explicated manually, increasing the complexity of glycomic studies. In this new developed method, no MS/MS data interpretation is required for structure identification, and all structural

identification is based on mass, retention time, and estimated NPSA. Dextrin, dextran and model glycans extracted from RNase B and Fetuin were used to investigate chromatographic behavior. Next, the glycans from HBS, a complex biological sample, were enzymatically released, reduced, permethylated, and purified by LC-MS. In total, 78 compositions were identified with mass accuracy less than 2 ppm. Most of the identified N-glycans from HBS fits the linear line of their own group. Also, when compared to estimated NPSAs, retention time can be used to predict N-glycan compositions, which can be used to differentiate between groups of structures with identical molecular weights. As these LC-MS procedures are further applied to glycomics studies, biomarker discovery will become largely simplified.

Acknowledgments

This work was supported by the office of the vice president for research at Texas Tech University and partially by an NIH grant (1R01 GM093322-01).

References

(1) Helenius, A.; Aebi, M. *Science* **2001**, *291*, 2364-2369.
(2) Rudd, P. M.; Elliott, T.; Cresswell, P.; Wilson, I. A.; Dwek, R. A. *Science* **2001**, *291*, 2370-2376.
(3) Dube, D. H.; Bertozzi, C. R. *Nat. Rev. Drug Discovery* **2005**, *4*, 477-488.
(4) Chen, C.; Schmilovitz-Weiss, H.; Liu, X.; Pappo, O.; Halpern, M.; Sulkes, O. J.; Braun, M.; Cohen, M.; Barak, N.; Tur-Kaspa, R.; Vanhooren, V.; Vlierberghe, H. V.; Libert, C.; Contreras, R.; Ben-Ari, Z. *J. Proteome Res.* **2009**, *8*.
(5) Goetz, J. A.; Mechref, Y.; Kang, P.; Jeng, M.; Novotny, M. V. *Glycoconj. J.* **2009**, *26*, 117-131.
(6) Mechref, Y.; Hussein, A.; Bekesova, S.; Pungpapong, V.; Zhang, M.; Dobrolecki, L. E.; Hickey, R. J.; Hammoud, Z. T.; Novotny, M. V. *J. Proteome Res.* **2009**, *8*, 2656-2666.
(7) Stanta, J. L.; Sadova, R.; Struwe, W. B.; Byrne, J. C.; Leweke, F. M.; Rothermund, M.; Rahmoune, H.; Levin, Y.; Guest, P. C.; Bahn, S.; Rudd, P. M. *J. Proteome Res.* **2010**, *9*, 4476-4489.
(8) Mechref, Y.; Novotny, M. V. *Anal. Chem.* **2003**, *75*, 4895-4903.
(9) Mechref, Y.; Kang, P.; Novotny, M. V. *Rapid Commun. Mass Spectrom.* **2006**, *20*, 1381-1389.
(10) Reinhold, V. N.; Reinhold, B. B.; Costello, C. E. *Anal. Chem.* **1995**, *67*, 1772-1784.
(11) Babu, P.; North, S. J.; Jang-Lee, J.; Chalabi, S.; Mackerness, K.; Stowell, S. R.; Cummings, R. D.; Rankin, S.; Dell, A.; Haslam, S. M. *Glycoconj J.* **2009**, *26*, 975-986.
(12) Wang, X.; Emmett, M. R.; Marshall, A. G. *Anal. Chem.* **2010**, *82*.
(13) Paschinger, K.; Razzazi-Fazeli, E.; Furukawac, K.; Wilsona, I. B. H. *J. Mass Spectrom.* **2011**, *46*.
(14) Rudd, P. M.; Colominas, C.; Royle, L.; Murphy, N.; Hart, E.; Merry, A. H.; Hebestreit, H. F.; Dwek, R. A. *Proteomics* **2001**, *1*, 285-294.
(15) Wuhrer, M.; Koeleman, C. A. M.; Deelder, A. M.; Hokke, C. H. *Anal. Chem.* **2004**, *76*, 833-838.
(16) Karlsson, N. G.; Schulz, B. L.; Packer, N. H.; Whitelock, J. M. *J. Chromatogr. B.* **2005**, *824*, 139-147.
(17) Wuhrer, M.; Geyer, H.; Ohe, M.; Gerardy-Schahn, R.; Schachner, M.; Geyer, R. *Biochimie.* **2003**, *85*, 207-218.
(18) Pabst, M.; Bondili, J. S.; Stadlmann, J.; Mach, L.; Altmann, F. *Anal. Chem.* **2007**, *79*, 5051-5057.
(19) Kang, P.; Mechref, Y.; Klouckova, I.; Novotny, M. V. *Rapid Commun. Mass Spectrom.* **2005**, *19*, 3421-3428.
(20) Kang, P.; Mechref, Y.; Novotny, M. V. *Rapid Commun. Mass Spectrom.* **2008**, *22*, 721-734.
(21) Mechref, Y.; Kang, P.; Novotny, M. V. *Methods Mol. Biol.* **2009**, *534*, 53-64.
(22) Nicholls, A.; Sharp, K. A.; Honig, B. *Proteins* **1991**, *11*, 281-296.
(23) Spolar, R. S.; Livingstone, J. R.; Record, M. T. J. *Biochemistry* **1992**, *31*, 3947-3955.
(24) Walker, S. H.; Papas, B. N.; Comins, D. L.; Muddiman, D. C. *Anal. chem.* **2010**, *82*, 6636-6642.
(25) Walker, S. H.; Lilley, L. M.; Enamorado, M. F.; Comins, D. L.; Muddiman, D. C. *J. Am. Soc. Mass spectrom.* **2011**, *22*, 1309-1317.

(26) Alley, J. W. R.; Madera, M.; Mechref, Y.; Novotny, M. V. *Anal. Chem.* **2010**, *82*, 5095-5106.
(27) Chu, C. S.; Niñonuevo, M. R.; Clowers, B. H.; Perkins, P. D.; An, H. J.; Yin, H.; Killeen, K.; Miyamoto, S.; Grimm, R.; Lebrilla, C. B. *Proteomics* **2009**, *9*, 1939-1951.
(28) Bereman, M. S.; Young, D. D.; Deiters, A.; Muddiman, D. C. *J. Proteome Res.* **2009**, *8*, 3764-3770.
(29) Bereman, M. S.; Williams, T.; Muddiman, D. C. *Anal. Chem.* **2009**, *81*, 1130-1136.
(30) Ruhaak, L. R.; C., H.; Waterreus, W.-J.; de Boer, A. R.; C., N.; Hokke, C. H.; Deelder, A. M.; Wuhrer, M. *Anal. Chem.* **2008**, *80*, 6119-6126.
(31) Stumpo, K. A.; Reinhold, V. N. *J. Proteome Res.* **2010**, *9*, 4823-4830.

Figure Legends

Figure 1. Comparison of retention time vs. glucose unit and NPSA vs. glucose unit of dextrin and N-glycans derived from fetuin.

Figure 2. Glycomic mapping of N-glycans derived from HBS (a). Linear fitting of the retention times of (b) high mannose; (c) complex-type biantennary; (d) complex-type triantennary; and (e) complex-type tetraantennary.

Figure 3. Linear plot of different glycan structures with each of the *m/z* values detected at two different retention times suggesting structural differences.

Figure 4. Tandem mass spectra of the ion observed at *m/z* value of 1079.225at retention times of (**a**) 31.95 min, and (**b**)33.76 min. and the ion at *m/z* value of 959.16 at retention times of (c) 25.93 min and (d) 27.5 min

Hu, Shihab and Mechref Figure 1

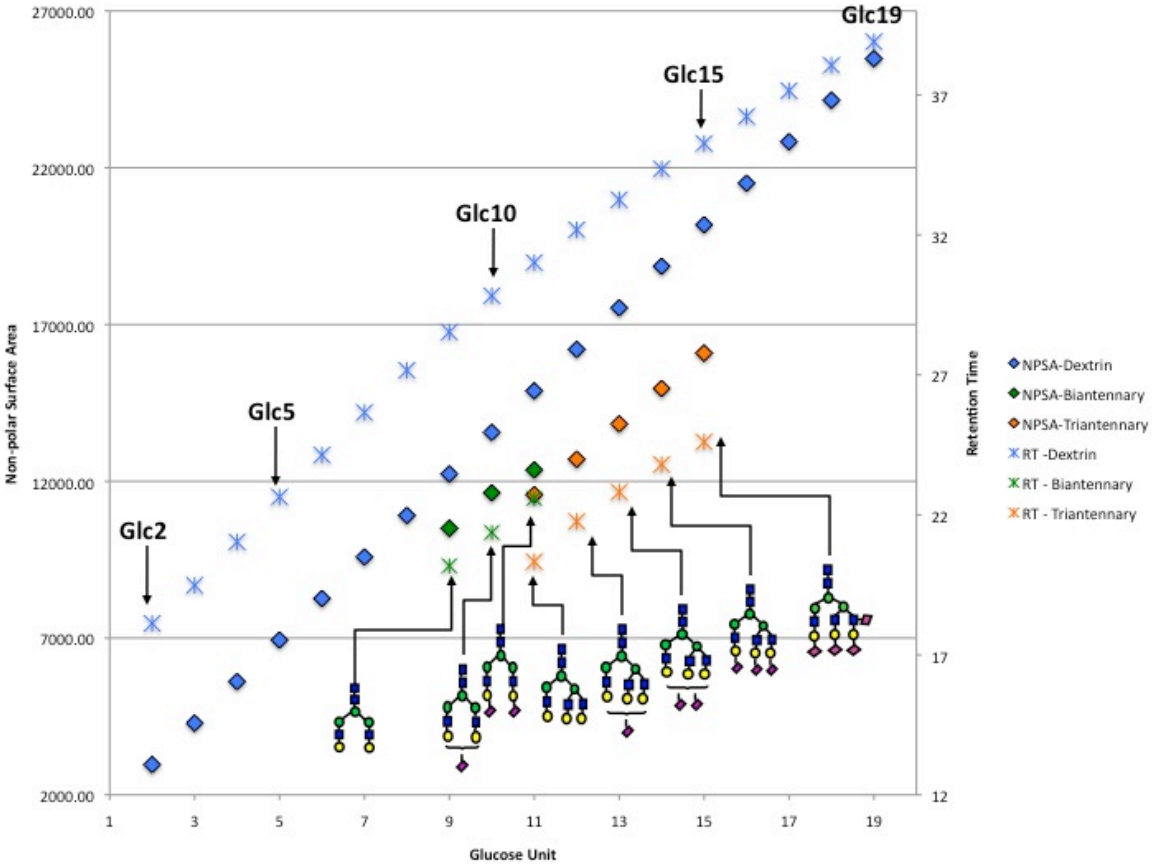

Hu, Shihab and Mechref Figure 2

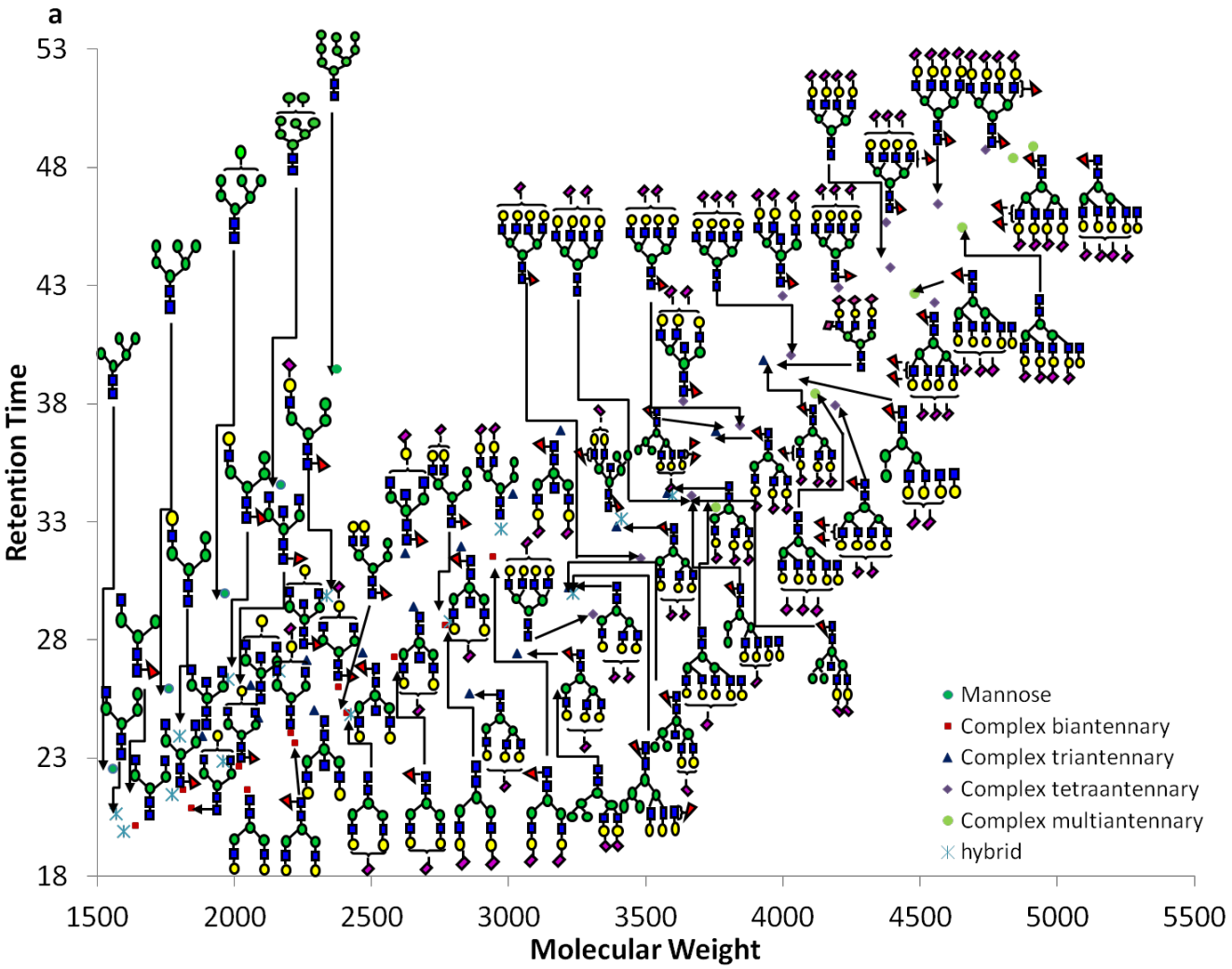

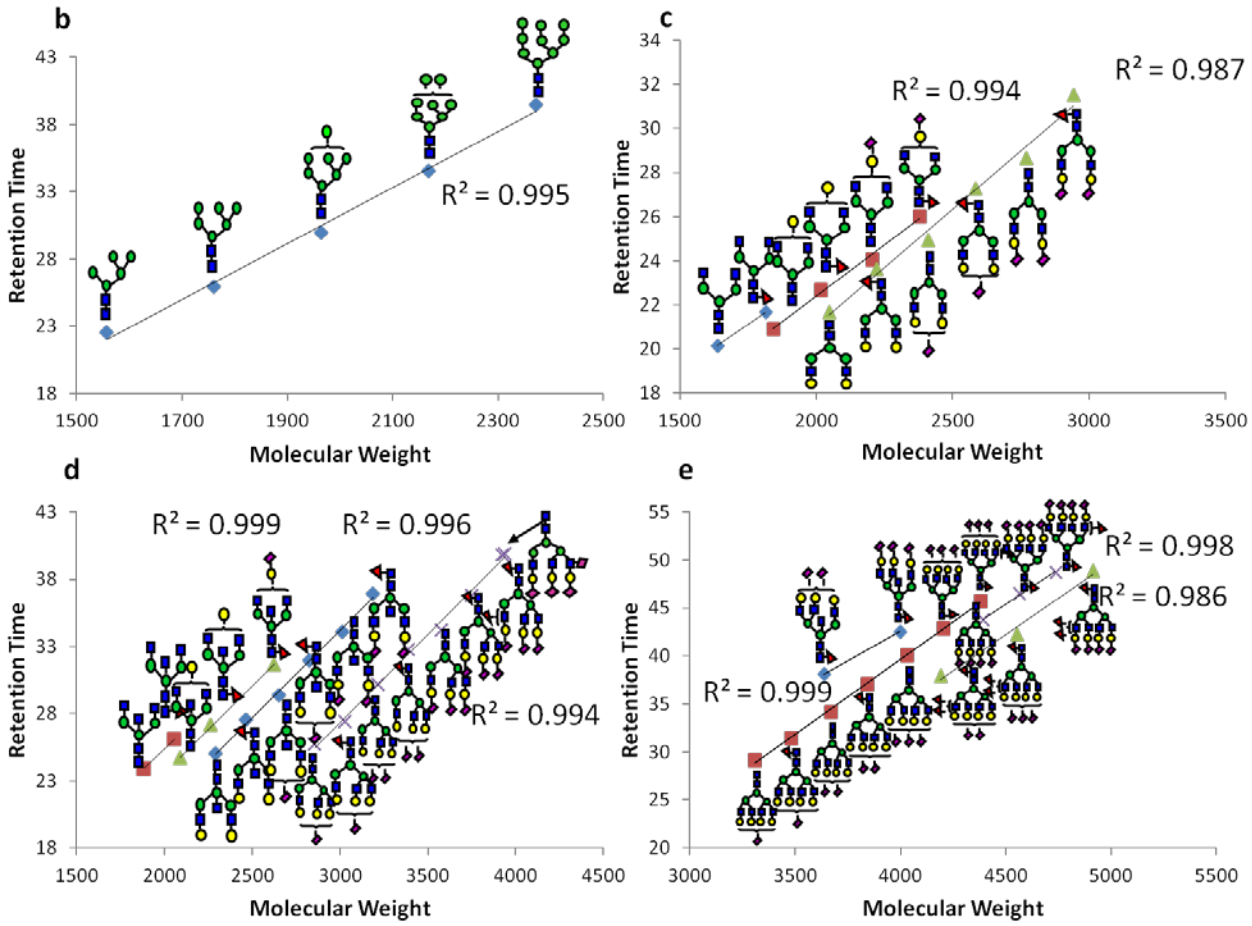
b
Retention Time
Molecular Weight
R² = 0.995
c
R² = 0.994
R² = 0.987
d
R² = 0.999
R² = 0.996
R² = 0.994
e
R² = 0.999
R² = 0.998
R² = 0.986

Hu, Shihab and Mechref Figure 3

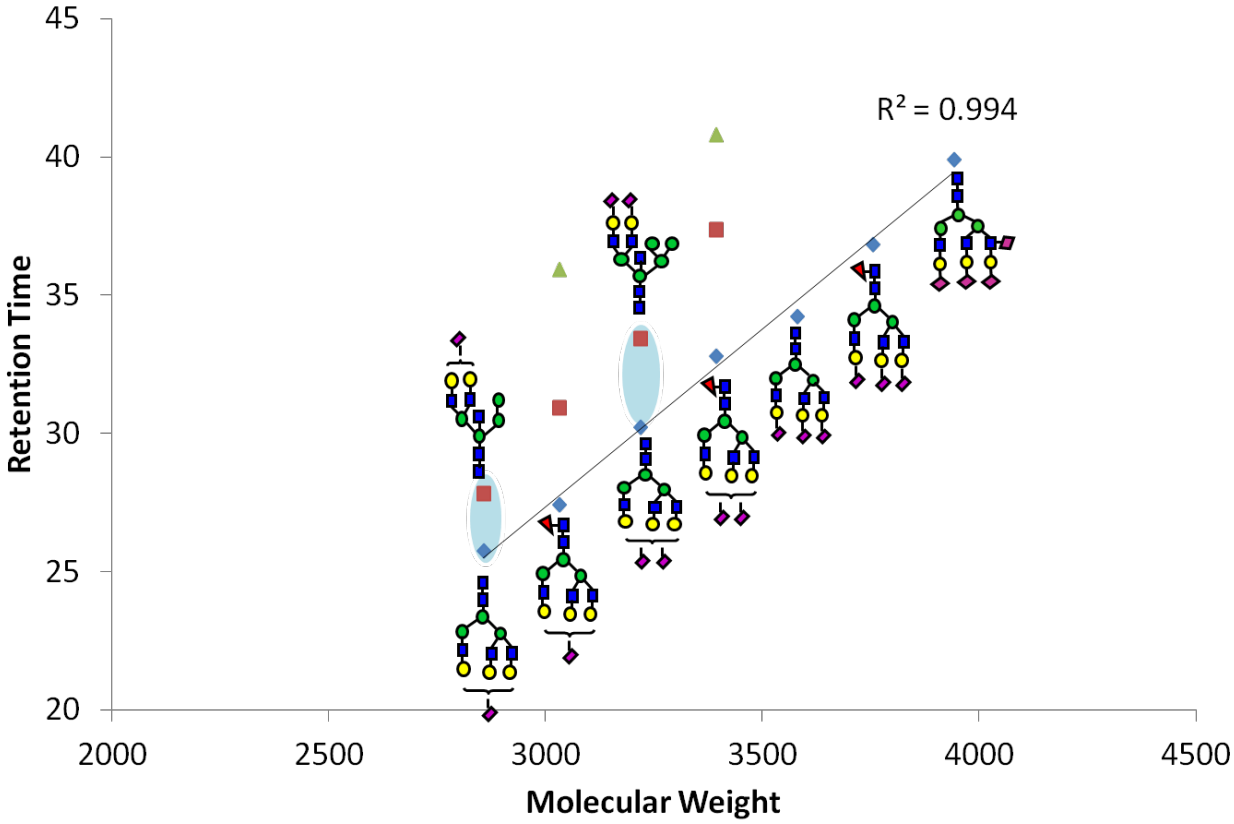

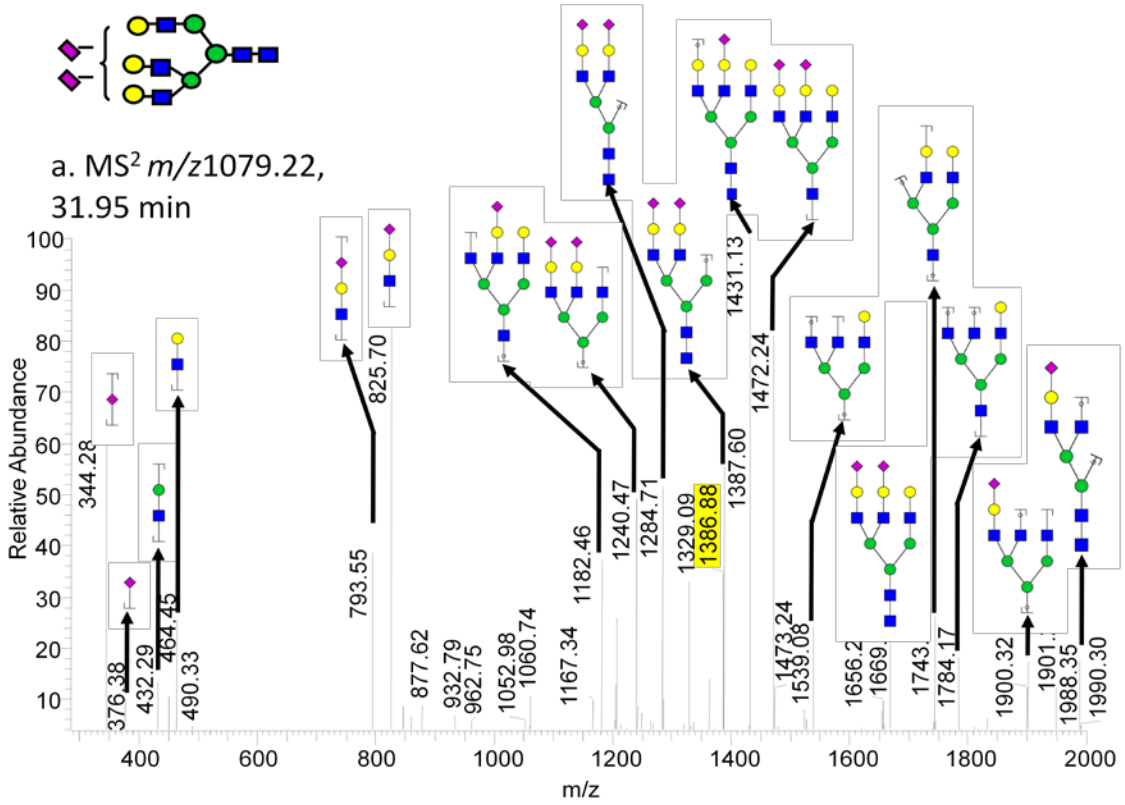
a. MS² m/z1079.22,
31.95 min
Relative Abundance
m/z
100
90
80
70
60
50
40
30
20
10
400
600
800
1000
1200
1400
1600
1800
2000
344.28
376.38
432.29
464.45
490.33
793.55
825.70
877.62
932.79
962.75
1052.98
1060.74
1167.34
1182.46
1240.47
1284.71
1329.09
1386.88
1387.60
1431.13
1472.24
1473.24
1539.08
1656.2
1669.
1743.
1784.17
1900.32
1901.
1988.35
1990.30

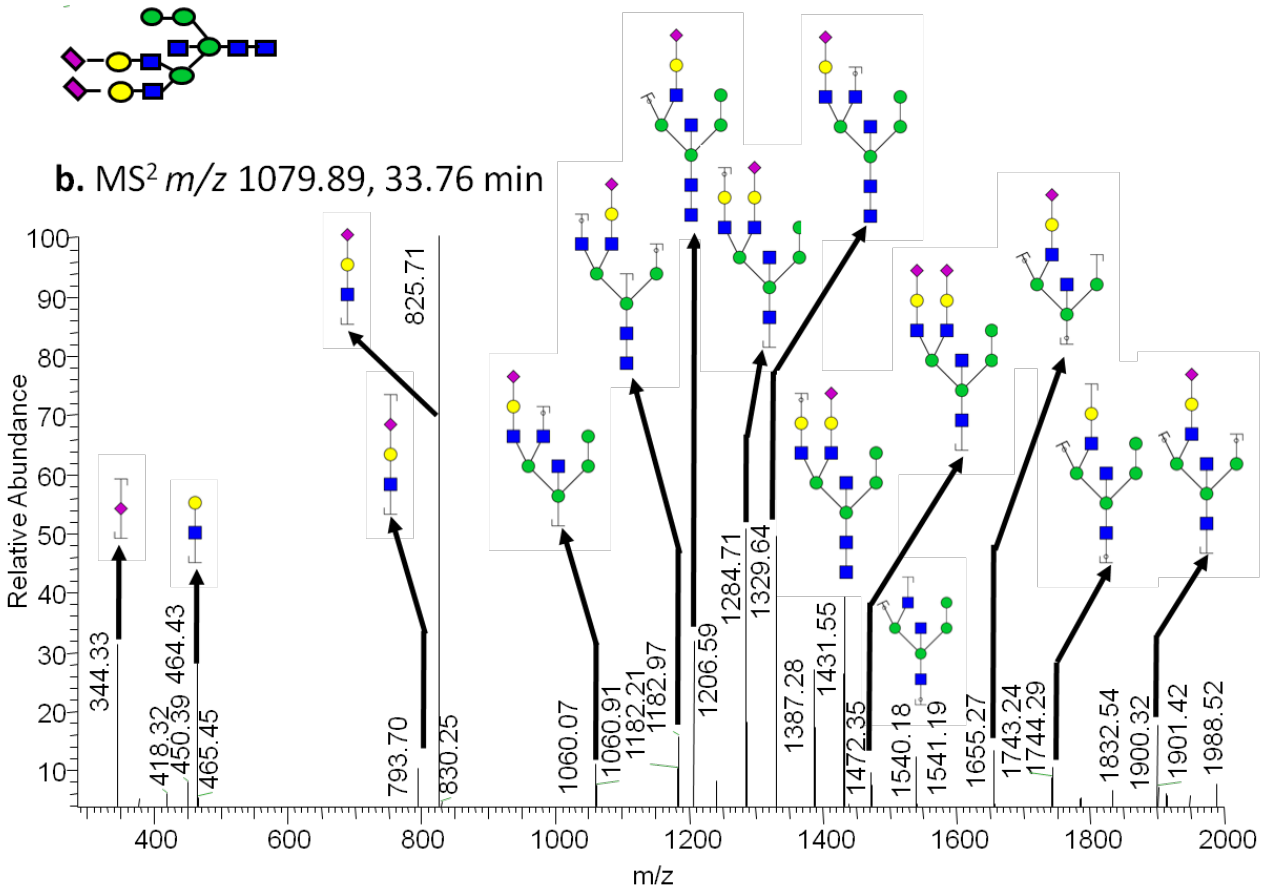
b. MS² m/z 1079.89, 33.76 min
Relative Abundance
m/z
344.33
418.32
450.39
464.43
465.45
793.70
825.71
830.25
1060.07
1060.91
1182.21
1182.97
1206.59
1284.71
1329.64
1387.28
1431.55
1472.35
1540.18
1541.19
1655.27
1743.24
1744.29
1832.54
1900.32
1901.42
1988.52

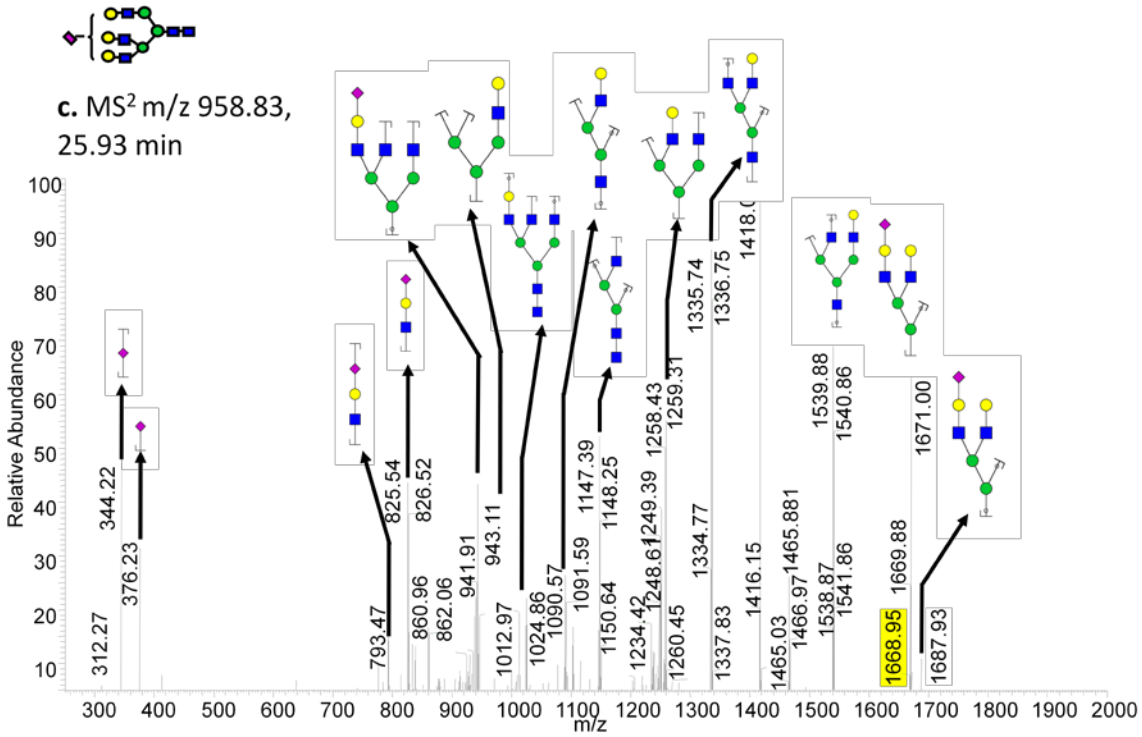
c. MS² m/z 958.83, 25.93 min
Relative Abundance
m/z
312.27
344.22
376.23
793.47
825.54
826.52
860.96
862.06
941.91
943.11
1012.97
1024.86
1090.57
1091.59
1147.39
1148.25
1150.64
1234.42
1248.61
1249.39
1258.43
1259.31
1260.45
1334.77
1335.74
1336.75
1337.83
1416.15
1418.(
1465.03
1465.881
1466.97
1538.87
1539.88
1540.86
1541.86
1668.95
1669.88
1671.00
1687.93

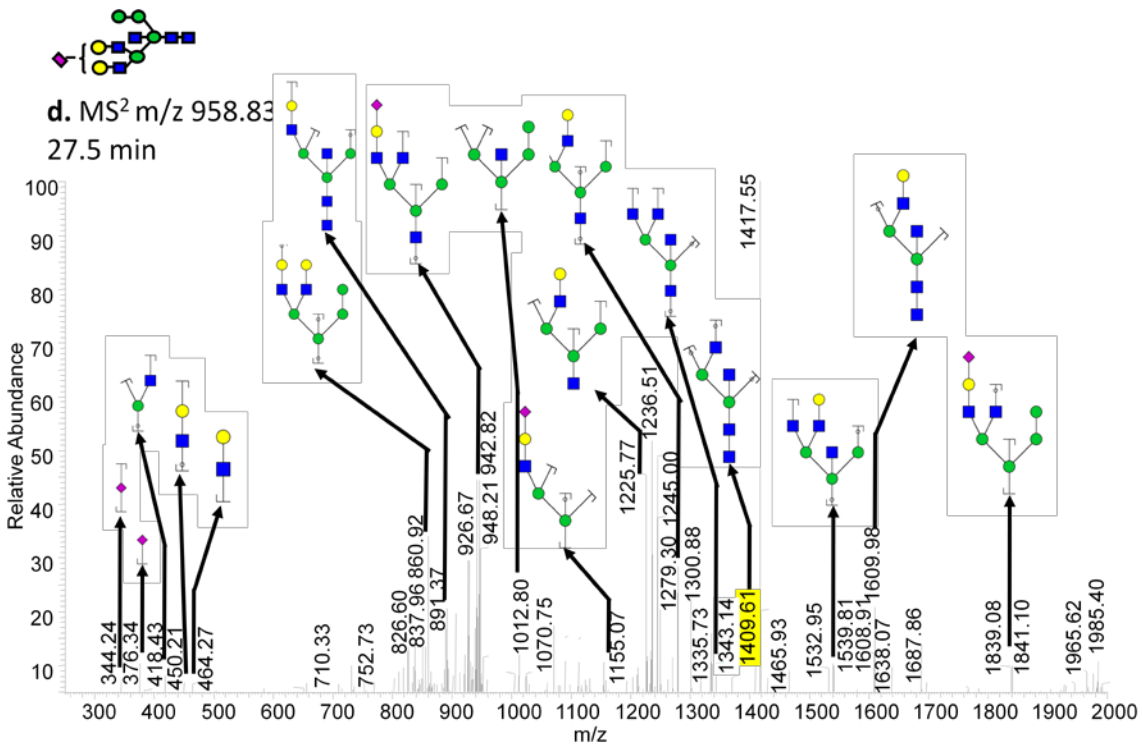
d. MS² m/z 958.83
27.5 min
Relative Abundance
m/z
344.24
376.34
418.43
450.21
464.27
710.33
752.73
826.60
837.96
860.92
891.37
926.67
942.82
948.21
1012.80
1070.75
1155.07
1225.77
1236.51
1245.00
1279.30
1300.88
1335.73
1343.14
1409.61
1417.55
1465.93
1532.95
1539.81
1608.91
1609.98
1638.07
1687.86
1839.08
1841.10
1965.62
1985.40